Clinical & Translational Immunology

Australian and New Zealand Society for Immunology Inc.

Clinical & Translational Immunology 2020; e1163. doi: 10.1002/cti2.1163
www.wileyonlinelibrary.com/journal/cti

ORIGINAL ARTICLE

Systematic analysis of disease-specific immunological signatures in patients with febrile illness from Saudi Arabia

Yiu-Wing Kam[1†], Mohamed Yousif Ahmed[1,2†], Siti Naqiah Amrun[1,3†], Bernett Lee[1], Tarik Refaie[2], Kamla Elgizouli[2], Siew-Wai Fong[1,3,4], Laurent Renia[1,3] & Lisa FP Ng[1,3,5,6,7]

[1]Singapore Immunology Network, Agency for Science, Technology and Research (A*STAR), Singapore
[2]Department of Infectious Diseases Clinic and Medical Microbiology, King Fahad Central Hospital, Jazan, Saudi Arabia
[3]Infectious Diseases Horizontal Technology Centre (ID HTC), Agency for Science, Technology and Research (A*STAR), Singapore
[4]Department of Biological Sciences, National University of Singapore, Singapore
[5]National Institute of Health Research, Health Protection Research Unit in Emerging and Zoonotic Infections, University of Liverpool, Liverpool, UK
[6]Institute of Infection, Veterinary and Ecological Sciences, University of Liverpool, Liverpool, UK
[7]Department of Biochemistry, Yong Loo Lin School of Medicine, National University of Singapore, Singapore

Correspondence
Lisa FP Ng, Laboratory of Microbial Immunity, Infectious Diseases Horizontal Technology Centre (ID HTC), and Singapore Immunology Network (SIgN), A*STAR, 8A Biomedical Grove, Immunos #04-06, Singapore 138648, Singapore.
E-mail: lisa_ng@immunol.a-star.edu.sg

[†]Equal contributors.

Received 9 March 2020;
Revised 9 June 2020;
Accepted 6 July 2020

doi: 10.1002/cti2.1163

Clinical & Translational Immunology
2020; **0**: e1163

Abstract

Objectives. Little is known about the prevalence of febrile illness in the Arabian region as clinical, laboratory and immunological profiling remains largely uncharacterised. **Methods.** A total of 2018 febrile patients from Jazan, Saudi Arabia, were recruited between 2014 and 2017. Patients were screened for dengue and chikungunya virus, *Plasmodium*, *Brucella*, *Neisseria meningitidis*, group A streptococcus and *Leptospira*. Clinical history and biochemical parameters from blood tests were collected. Patient sera of selected disease-confirmed infections were quantified for immune mediators by multiplex microbead-based immunoassays. **Results.** Approximately 20% of febrile patients were tested positive for one of the pathogens, and they presented overlapping clinical and laboratory parameters. Nonetheless, eight disease-specific immune mediators were identified as potential biomarkers for dengue (MIP-1α, MCP-1), malaria (TNF-α), streptococcal and meningococcal (eotaxin, GRO-α, RANTES, SDF-1α and PIGF-1) infections, with high specificity and sensitivity profiles. Notably, based on the conditional inference model, six of these mediators (MIP-1α, TNF-α, GRO-α, RANTES, SDF-1α and PIGF-1) were revealed to be 68.4% accurate in diagnosing different febrile infections, including those of unknown diseases. **Conclusions.** This study is the first extensive characterisation of the clinical analysis and immune biomarkers of several clinically important febrile infections in Saudi Arabia. Importantly, an immune signature with robust accuracy, specificity and sensitivity in differentiating several febrile infections was identified, providing useful insights into patient disease management in the Arabian Peninsula.

Keywords: biomarkers, cytokines, infectious diseases, patients, Saudi Arabia

INTRODUCTION

The Kingdom of Saudi Arabia hosts annual Islamic religious events that attract millions of pilgrims worldwide.[1,2] The constant human movement puts the region in a unique and vulnerable position, where the risk of import and export of communicable diseases can lead to the spread of global outbreaks.[1,2]

Several bacterial infections are endemic in Saudi Arabia, including brucellosis and meningococcal diseases caused by the Gram-negative *Brucella* and *Neisseria meningitidis*, respectively.[3–7] Human movement and the importation of significant numbers of livestock during the Hajj season are reasons for endemicity,[3,6–8] high morbidity and mortality rates.[4,7] Similarly, group A streptococcus (GAS) or dominantly *Streptococcus pyogenes* infections have high mortality rates of 20%.[9–11] Over the past decades, invasive and severe manifestations of GAS infections have occurred more frequently, likely because of the emergence of new virulent strains.[9,12] Leptospirosis, caused by spirochaete *Leptospira* species, can also present a diverse range of symptoms in humans, including meningitis, pulmonary haemorrhage and death.[13,14] Given the wide spectrum of clinical presentations, the incidence of leptospirosis in Saudi Arabia is likely to be underestimated.[15]

Vector-borne infectious diseases have gained prominence in recent years as a result of recurring outbreaks, especially in the tropics and subtropics.[16,17] The climate of Saudi Arabia favors breeding of *Anopheles* and *Aedes* mosquitoes, the arthropod vectors responsible for the transmission of protozoan parasite *Plasmodium* species, and dengue (DENV) and chikungunya (CHIKV) viruses.[2,16] Malaria, caused by the protozoan parasite *Plasmodium*, is mostly concentrated in the south-western parts of Saudi Arabia, Aseer and Jazan.[18,19] While malaria has been reported in Saudi Arabia since the 1940s,[20] DENV and CHIKV emerged only recently. The first DENV outbreak in Saudi Arabia was in 1994 with 289 confirmed cases,[21,22] while the first autochthonous case of CHIKV infection was in 2013.[23]

The clinical symptoms and manifestations presented by these tropical diseases are common and indistinguishable, thus making differential diagnosis difficult.[24,25] Laboratory tests are therefore required to make a confirmatory diagnosis, but often, these are unavailable or too expensive in developing countries.[25,26] In this study, we first characterised the clinical and laboratory parameters of febrile diagnosed patients from Jazan, Saudi Arabia. Comprehensive multiplex microbead-based assays were performed to identify specific immune mediators associated with the disease. This study thus provides an in-depth profiling of disease prevalence in Saudi Arabia, revealing key predictors of pathogen-specific infections that can aid in improving the current practices of clinical management in the region and elsewhere. This is especially so in the current ongoing coronavirus disease 2019 (COVID-19) outbreak[27] in which febrile patients present overlapping symptoms.

RESULTS

One-fifth of febrile illnesses are known pathogen infections

Between January 2014 and December 2017, 2018 symptomatic patients visited the clinic and were recruited into the study upon hospital admission. All febrile patients' sera (median sampling day of 3 days post-illness onset) were screened by qRT-PCR, serology ELISAs or bacterial culturing methods for pathogen identification. Only 401 patients, or 19.9% of the cohort, were diagnosed for at least one of the seven pathogens tested (Table 1). A majority of the diagnosed cases was because of DENV (42.4%), followed by GAS (16.7%), *Plasmodium* (13.2%) and *N. meningitidis* (13.0%) (Table 1). CHIKV, DENV-CHIKV co-infection, *Brucella* and *Leptospira* infections accounted for $< 10\%$ of the total diagnosed cases (Table 1). Given that there were only two cases of leptospirosis throughout the 4 years of recruitment, this group was excluded from further analysis in subsequent sections.

Plasmodium infections display seasonal variation

From 2014 to 2017, cases of DENV, *Plasmodium*, *N. meningitidis* and GAS infections were recorded throughout the years with a stable frequency (Figure 1a). However, a surge of CHIKV cases was observed in mid-2014 and declined in 2015, with no reported cases until the end of the study (Figure 1a). Naturally, a similar trend was observed for DENV-CHIKV co-infections (Figure 1a). Conversely, *Brucella* infections occurred sporadically over the years with no clear trend (Figure 1a). Notably, incidences

Table 1. Demographics and clinical characteristics of patients from Saudi Arabia with febrile known infections

	Febrile infections								
Parameters	DENV	CHIKV	DENV-CHIKV co-infection	*Plasmodium*	*Brucella*	*Neisseria meningitidis*	GAS	*Leptospira*	Healthy controls
Number of patients, *N*	170	34	15	53	8	52	67	2	31
Percentage of cases (%)	42.4	8.5	3.7	13.2	2.0	13.0	16.7	0.5	N.A.
Age, median (range), years	26 (14–70)	47 (31–69)	56 (29–65)	31 (15–63)	46 (33–50)	45 (18–75)	59 (20–75)	52 (43–60)	41 (21–63)
Gender ratio (male/female)	1.2 (93M/77F)	1.1 (18M/16F)	2 (10M/5F)	0.9 (25M/28F)	7 (7M/1F)	1.6 (32M/20F)	1.5 (40M/27F)	(2M/0F)	0.8 (14M/17F)
Fever (%)	100	100	100	100	100	100	100	100	0
Rash (%)	99.4	100	93.3	1.9	0	73.1	11.9	100	0
Back pain (%)	82.4	64.7	100	83	100	69.2	83.6	0	0
Headache (%)	62.9	100	86.7	100	100	100	89.6	100	0
Joint pain (%)	97.1	100	100	54.7	100	53.9	64.2	0	0
Vomiting (%)	71.2	35.3	100	71.7	25	92.3	80.6	100	0
Nausea (%)	90.6	61.8	100	98.1	37.5	100	95.5	100	0
Chills (%)	98.2	100	100	98.1	12.5	63.5	73.1	100	0
Neutrophils, mean (%)	36.1 ± 5.4	45.2 ± 6.6	31.5 ± 4.5	58.1 ± 11.9	42.1 ± 6.9	90.1 ± 4.9	87.8 ± 8	74 ± 8.5	58.6 ± 5.3
Lymphocytes, mean (%)	15.8 ± 3.0	15.2 ± 2.5	13 ± 1.3	31.1 ± 4.4	21.9 ± 6.3	48.2 ± 8.7	46.4 ± 9.4	47.5 ± 3.5	33.5 ± 3.8
Erythrocyte sedimentation rate (ESR), mean ($mm\ h^{-1}$)	11.2 ± 4.9	11.8 ± 4.5	17.7 ± 7.8	11.2 ± 5.8	31.9 ± 18.2	20.2 ± 8.5	23.5 ± 10	24.5 ± 9.2	12.5 ± 3.3
Haemoglobin, mean ($g\ dL^{-1}$)	11.9 ± 1.0	12 ± 0.9	10.5 ± 0.8	12.5 ± 1.1	11.3 ± 1	12 ± 1.0	12.1 ± 1.1	11.5 ± 0.7	13.5 ± 0.9
Platelet *1000	95.9 ± 14.7	274.7 ± 67.2	78.2 ± 10.8	195 ± 76.6	211.4 ± 113.3	422.3 ± 134	439.8 ± 121.8	268.5 ± 78.5	342.9 ± 48.5
Alanine aminotransferase (ALT), mean	75.2 ± 21.2	42.9 ± 2.6	102.9 ± 7.2	43.4 ± 5.6	85.8 ± 16.5	42.9 ± 5.4	40.5 ± 6.9	103.5 ± 13.4	31.3 ± 7.2
Aspartate aminotransferase (AST), mean	64 ± 20.1	31.2 ± 4.2	91.3 ± 7.1	33 ± 6.1	73.8 ± 16.2	32.2 ± 3.7	30.6 ± 5	90.5 ± 6.4	27.3 ± 5.7
C-reactive protein (CRP), mean ($mg\ dL^{-1}$)	28.9 ± 8.9	20.2 ± 7.4	34.9 ± 8.1	23.4 ± 13	46.8 ± 17.6	74.7 ± 36.4	83.4 ± 40.5	36 ± 29.7	4.8 ± 0.9

of malaria demonstrated a seasonal pattern. *Plasmodium* infections were higher in the months ranging from May to October each year (Figure 1a), coinciding with higher temperatures in Jazan (Supplementary figure 1a).

Acute febrile infections present overlapping clinical and laboratory parameters

Reported clinical symptoms were next analysed and compared (Figure 1b and Table 1). With the exception of brucellosis, all other febrile infections largely showed overlapping clinical manifestations, such as headache, chills and back and joint pains (Figure 1b and Table 1). However, rashes were only observed in few *Plasmodium*- and GAS-infected patients (1.9% and 11.9% cases, respectively; Figure 1b and Table 1). Furthermore, patients with DENV-CHIKV co-infections reported more symptoms such as vomiting, nausea and back pain, than the single virus infections during the hospital admission period (Figure 1b and Table 1).

Majority of the medical laboratory parameters recorded from febrile patients in this cohort did not show disease-specific patterns (Figure 2). In terms of immune cell profiling, the percentage of

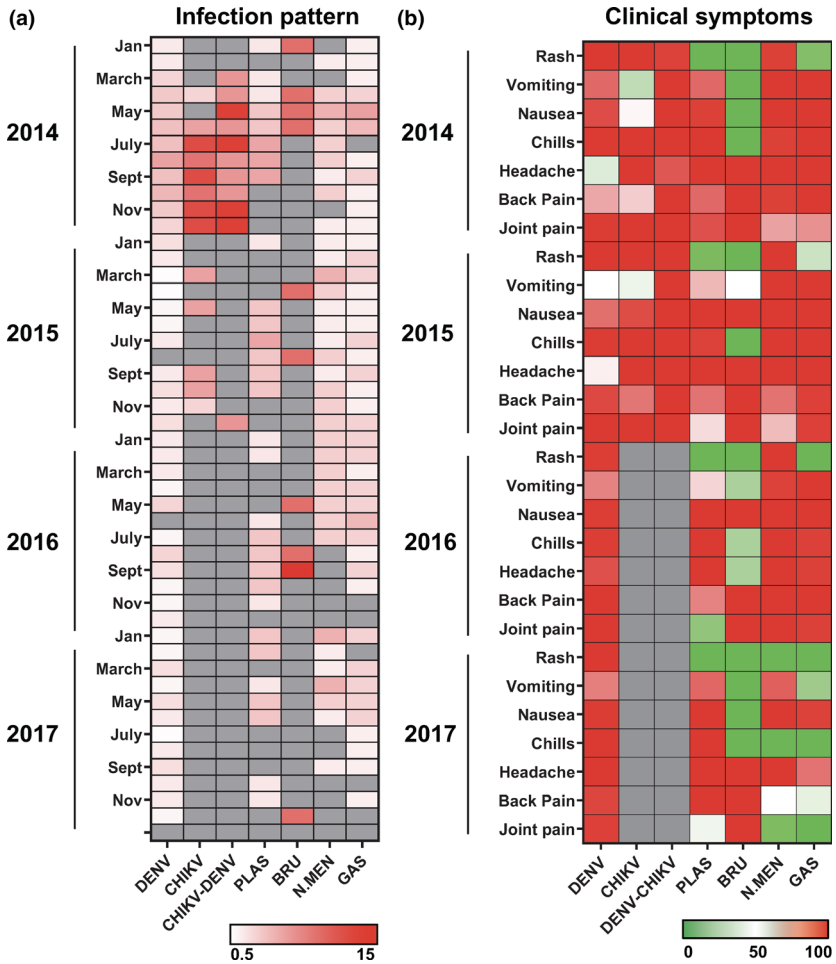

Figure 1. Longitudinal pattern of disease cases and clinical parameters of febrile diagnosed patients during the acute phase of disease. **(a)** Percentage of positively diagnosed cases between 2014 and 2017 (n = 401) collected in Jazan, Saudi Arabia. Data were expressed as percentage of disease-specific [(number of disease-specific cases per month/total number of disease-specific cases between 2014 and 2017) × 100%] and presented in a heatmap format, with white and red colours representing low and high percentage of cases, respectively. Grey colour indicates no disease cases. **(b)** Clinical parameters reported during the acute phase of disease (within 7 days post-illness onset) were analysed and presented in a heatmap of normalised scores. In the heatmap, patients were grouped according to the collection time (year) and the clinical parameters were scaled between 0 in green (minimum) and 100 in red (maximum) for each recorded clinical parameter of the respective disease group. Grey colour indicates no reports of clinical symptoms.

neutrophils showed opposing trend between viral and bacterial infections (Figure 2a). Compared to the healthy controls, DENV and DENV-CHIKV co-infections showed a significant reduction in neutrophil population, while infections with *N. meningitidis* and GAS showed a significant increase (Figure 2a). Interestingly, brucellosis cases presented a similar neutrophil profile as the viral infections, and no differences were reported between malaria patients and the healthy controls (Figure 2a). A similar trend was also observed for the percentage of lymphocytes in this cohort (Figure 2b), while platelet counts decreased significantly only for DENV, DENV-CHIKV and malaria cases (Figure 2c). In terms of haematological parameters, levels of nonspecific inflammation parameter erythrocyte sedimentation rate (ESR) were significantly high for all bacterial infection cases (Figure 2d) whereas infections with any of the seven pathogens would cause a significant decrease in haemoglobin content (Figure 2e). In terms of liver inflammation markers, the levels of C-reactive protein (CRP) and alanine aminotransferase (ALT) significantly increased in all of the studied diseases (Figure 2f and g). However, levels of aspartate aminotransferase (AST) increased significantly only for DENV, DENV-CHIKV and brucellosis cases (Figure 2h).

Cytokine responses vary for different febrile infections

In order to identify and define disease-specific immune mediators, serum samples of healthy controls and DENV-, *Plasmodium*-, *N. meningitidis*- and GAS-infected febrile patients were subjected to a multiplex microbead-based immunoassay. The remaining diseases were excluded because of insufficient sample size and sera availability. Twenty-four out of 45 immune mediators did not show any significant differences between the disease groups and healthy controls (Figure 3a and Supplementary table 1). Levels of 10 other factors [interferon IFN-γ, interleukins IL-6, IL-7, IL-18, IL-10, IL-1RA, interferon-γ-induced protein 10 kDa (IP-10), platelet-derived growth factor-BB (PDGF-BB), brain-derived neurotrophic factor (BDNF) and epidermal growth factor (EGF)] demonstrated significant differences in more than one group of patients when compared to healthy controls (Figure 3a and Supplementary figure 2). Only eight immune mediators [macrophage inflammatory protein-1α (MIP-1α), monocyte chemoattractant protein-1 (MCP-1), tumor necrosis factor-α (TNF-α), growth-regulated oncogene-α (GRO-α), regulated on activation, normal T cell expressed and secreted (RANTES), eotaxin, stromal cell-derived factor-1α (SDF-1α) and placental growth factor-1 (PIGF-1)] showed disease-specific profiles that were significantly different from the healthy controls and also distinct from other infection groups (Figure 3b). DENV- and *Plasmodium*-infected patients showed elevated levels of MIP-1α and MCP-1, and TNF-α, respectively (Figure 3b). In contrast, GRO-α, RANTES, eotaxin, SDF-1α and PIGF-1 were significantly decreased in the sera of *N. meningitidis*- and GAS-infected patients (Figure 3b).

To further evaluate the robustness of these selected immune mediators as disease-specific biomarkers, receiver operating characteristic (ROC) analysis was performed. The eight immune mediators showed high area under curve (AUC), and specificity and sensitivity values in disease prediction (Table 2). Remarkably, RANTES for *N. meningitidis* and GAS infections had the best specificity (0.968) and sensitivity (0.923 and 1.000) profile (Table 2). Altogether, a combination of cytokines and chemokines can be used in tandem to act as robust biomarkers to positively predict diseases with indistinguishable clinical presentations (Figure 3c).

Immune signature for differential diagnosis of febrile infections

In order to further evaluate the performance of the potential biomarkers identified, a multivariate analysis was performed. To ensure a more robust prediction, the levels of eight immune mediators from 30 patients with febrile unknown infections were also interrogated (Supplementary table 2). Conditional inference analysis with 10-fold cross-validation yielded an optimal signature composing of six cytokines, MIP-1α, TNF-α, GRO-α, RANTES, SDF-1α and PIGF-1, with a high accuracy of 68.4% (Figure 4a). Patients showing serum concentrations (Log_{10} scale, pg mL^{-1}) between -0.255 and 1.701 for RANTES were likely to be infected with *N. meningitidis* or GAS (80.4% probability), whereas patients with $>$ 1.701 for RANTES, $>$1.029 for GRO-α and $\leq$ 0.825 for TNF-α were most likely suffering from DENV infections (88.9% probability; Figure 4a). In contrast, those with $>$ 0.825 for TNF-α and MIP-1α concentrations between 0.648 and 1.733 could be *Plasmodium*-infected (71.4% probability), and patients with GRO-α concentration of $\leq$ 1.029 and

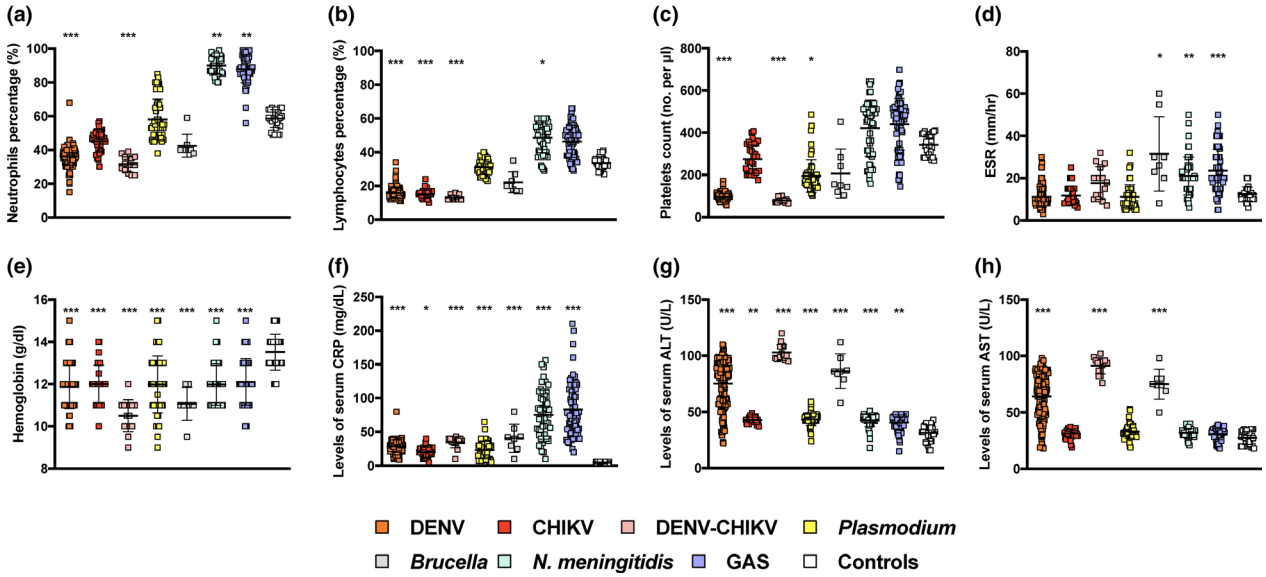

Figure 2. Laboratory parameter profiles of febrile diagnosed patients during the acute phase of the disease. Blood and serum samples of healthy controls (n = 31) and patients infected with DENV (n = 170), CHIKV (n = 34), DENV-CHIKV co-infection (n = 15), *Plasmodium* (n = 53), *Brucella* (n = 8), *Neisseria meningitidis* (n = 52) or GAS (n = 67) at acute phase (within 7 days post-illness onset) were tested for **(a–c)** levels of blood cells and platelets, **(d, e)** haematological parameters and **(f–h)** liver inflammation markers. Results are depicted as dot plots with mean ± SD, and statistical analysis between disease groups and healthy controls was conducted with Kruskal–Wallis test with Dunn's post hoc tests (*P < 0.05, **P < 0.01, ***P < 0.001).

RANTES concentration of > 2.153 were likely to be infected with febrile diseases distinct from these four pathogens (68.4% probability; Figure 4a).

The serum levels of the six cytokines from conditional inference tree were then used to build an immune signature, and the radar plot revealed clear differential profiles among the four groups of febrile diseases (Figure 4b). In this cohort, DENV infections induced high levels of GRO-α, MIP-1α, PIGF-1, RANTES and SDF-1α, but low levels of TNF-α (Figure 4b). However, *Plasmodium* infections showed the opposite phenomenon, while bacterial infections presented even lower levels of these cytokines (Figure 4b). Interestingly, febrile unknown infections showed an intermediate response of the six cytokines (Figure 4b).

DISCUSSION

Infectious diseases represent one of the global causes of morbidity and mortality,[1] with vector-borne diseases garnering increased attention because of the emergence of pathogens.[1,17] Indeed, arthropod-borne infections accounted for 67.8% of the febrile cases in this cohort, with majority being DENV. Although DENV transmission is generally reported to be sensitive to environmental factors,[28] the number of DENV cases was constant throughout the study period despite changes in temperature, humidity and rainfall (Supplementary figure 1). Instead, seasonality was observed for malaria, and it has been shown that changes in temperature control the *Anopheles* mosquito life cycle and parasite development, thus regulating disease transmission.[29] This suggests that the activity of different vectors and pathogens could be regulated by environmental factors at different levels, and understanding the dynamics of climate and vector is important in the effective planning and implementation of routine control measures.[28]

Because of the similar clinical presentations and overlapping endemicity of malaria, DENV and CHIKV infections in tropical regions, simultaneous infections with more than one of the pathogen are very likely to be underreported and misdiagnosed as a mono-infection.[16] DENV-CHIKV co-infections have been described in 26 different countries, including Yemen.[16,30,31] To our knowledge, this is the first report showing the incidence of DENV-CHIKV co-infections in Saudi Arabia. Interaction of multiple pathogens can potentially lead to different outcomes[16] and this was observed clinically in our study, as well as in a cohort in Bengal, India, in which the co-infected patients experienced more symptoms than those with single infections.[32] Furthermore, the laboratory parameters of DENV-

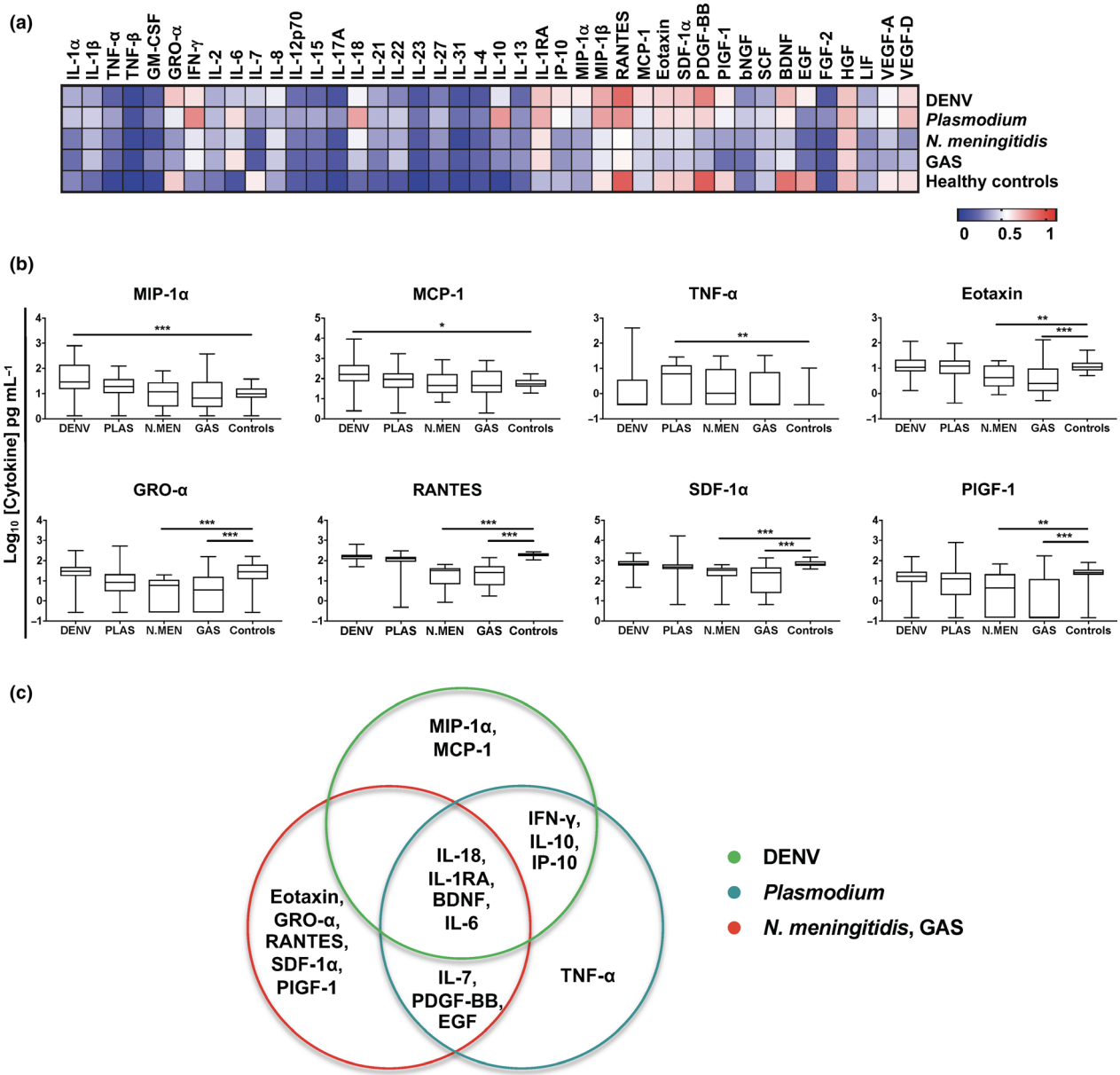

Figure 3. Immune signature for differential diagnosis of febrile infections during the acute phase of disease. Serum samples of healthy controls (n = 31) and patients infected with DENV (n = 100), *Plasmodium* (PLAS; n = 30), *Neisseria meningitidis* (N.MEN; n = 21), group A streptococcus (GAS; n = 26) or febrile unknown (n = 30) at acute phase (within 7 days post-illness onset) were subjected to multiplex microbead-based immunoassay. **(a)** Levels of immune mediators were analysed and presented in a heatmap of normalised scores. The concentrations of each immune mediator were scaled between 0 and 1, and the average scaled value was computed for each group. **(b)** Selected immune mediators with disease-specific profiles are depicted as Tukey box plots with the results of post hoc t-tests shown as asterisks. One-way ANOVAs were conducted on the logarithmically transformed concentration with post hoc t-tests corrected using the method of Bonferroni. ANOVA results were corrected for multiple testing using the method of Benjamini and Hochberg (*P < 0.05, **P < 0.01, ***P < 0.001). Data in **b** and **c** are of one independent experiment. **(c)** Immune mediator signature profiles of febrile patients in the acute phase of disease. Venn diagram shows the generic febrile and virus-specific immune mediators for each infection compared to healthy controls.

CHIKV co-infected patients, such as neutrophil percentage, platelet count and levels of serum AST and ALT, resembled closely to those of DENV infections rather than CHIKV (Figure 2) and were similarly observed in co-infected patients in India.[33] Although DENV–malaria, CHIKV–malaria and DENV–CHIKV–malaria co-infections have been demonstrated elsewhere,[16] none of the different

Table 2. Receiver operating characteristic (ROC) analysis of biomarkers

	Immune mediator	Infection	Area under curve	Specificity	Sensitivity
Virus	MIP-1α	DENV	0.814	0.774	0.730
	MCP-1	DENV	0.769	0.903	0.580
Parasite	TNF-α	*Plasmodium*	0.811	0.935	0.633
Bacteria	Eotaxin	*Neisseria meningitidis*	0.740	0.935	0.619
	Eotaxin	GAS	0.779	1.000	0.692
	GRO-α	*Neisseria meningitidis*	0.866	0.806	0.762
	GRO-α	GAS	0.804	0.774	0.731
	RANTES	*Neisseria meningitidis*	0.998	0.968	1.000
	RANTES	GAS	0.970	0.968	0.923
	SDF-1α	*Neisseria meningitidis*	0.860	0.677	0.905
	SDF-1α	GAS	0.793	0.903	0.731
	PIGF-1	*Neisseria meningitidis*	0.729	0.871	0.714
	PIGF-1	GAS	0.847	0.935	0.731

combinations was detected in this study. Given the limited knowledge on concurrent infections, more investigations are required to understand the interplay of different pathogens on the host immune system and pathogenesis.

Consistent with previous reports, low platelet levels were found in DENV patients,[34,35] while patients suffering from bacterial infections had significantly high level of circulating neutrophils.[36,37] However, other laboratory markers did not show any disease specificity. Infections with any of the pathogens induced a systematic inflammation in patients, as indicated by elevated serum levels of CRP and ALT (Figure 2f and g). Overall, laboratory parameters are not distinctive in predicting pathogen-specific infections in febrile patients, thus warranting an in-depth biomarker identification in this study.

In this cohort, infections with any pathogen triggered a common response of inflammatory cytokines. Elevated levels of anti-inflammatory IL-1RA, pro-inflammatory IL-18 and IL-6, as well as decreased BDNF level, were observed, and data were mostly congruent with previous reports for DENV and malaria.[38,39] Nonetheless, disease-specific biomarkers for dengue, malaria and bacterial infections were identified. MIP-1α and MCP-1 were found to be dengue-specific, as reported in previous studies.[40–42] TNF-α, however, is a unique identifier of malaria in this cohort, correlating well with previous studies reporting increased TNF-α levels in *Plasmodium vivax* and *Plasmodium falciparum* infections.[43,44] For patients with *N. meningitidis* and GAS infections, decreased concentrations of eotaxin, GRO-α, RANTES, SDF-1α and PIGF-1 were observed, and these mediators play integral roles in host immune response to bacterial infection.[45–49]

This study has identified a signature of six immune mediators that could accurately distinguish DENV, *Plasmodium*, and *N. meningitidis* or GAS infections. Specifically, with the ongoing COVID-19 outbreaks,[27] the symptom overlap in febrile illness underscores the necessity of completing a differential diagnosis for all patients globally. With the current knowledge that severe acute respiratory syndrome coronavirus 2 (SARS-CoV-2) infection triggers a cytokine storm with markedly increased levels of generic febrile immune mediators IL-6, IL-1RA and IL-18 in COVID-19 patients,[50–53] the pathogen-specific immune mediators identified in this study will be useful in effective patient stratification during this uncontrolled COVID-19 outbreak. Nonetheless, more investigations are required to determine the classification power of the immune signature and how they can be implemented in the diagnosis practice in hospitals in the Arabian Peninsula. Taken together, the combination of clinical observations and profiles of laboratory parameters as well as the detection of disease-specific immune mediators can aid in the differential diagnosis of febrile patients. This will thus greatly improve the accuracy of disease prediction, alleviating the burden placed on the public health system. Moreover, to prepare for future outbreaks, the health authorities in Saudi Arabia could implement new strategies to better forecast the evolving trends of infectious diseases.

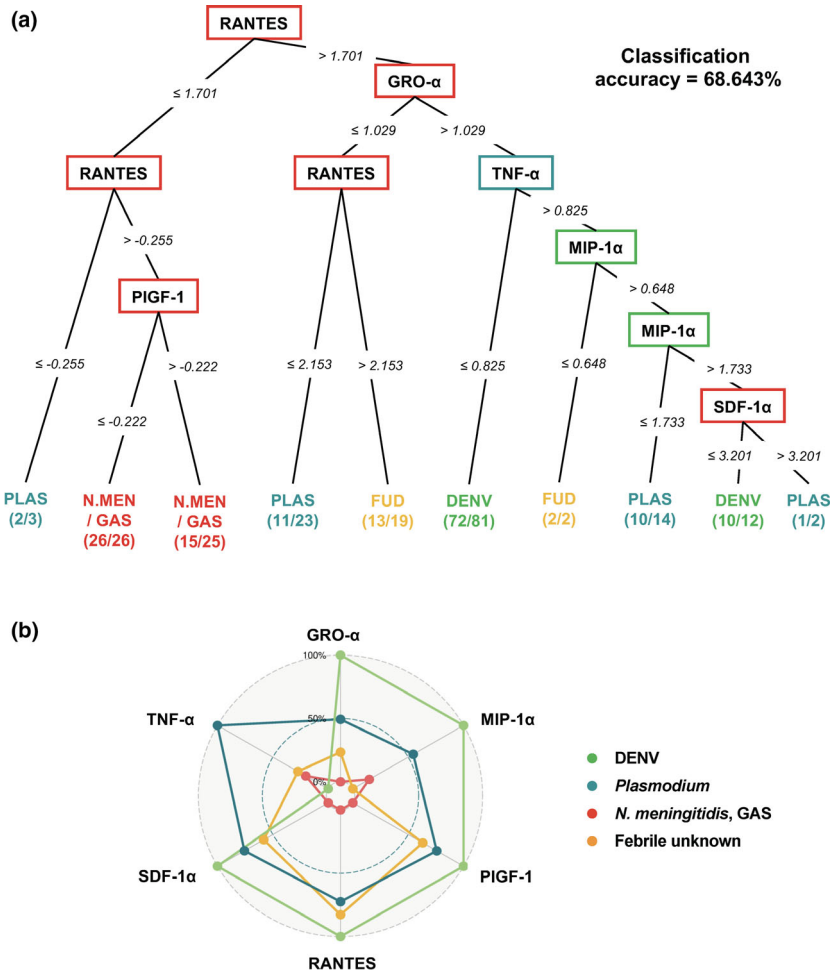

Figure 4. Multivariate analysis of immune mediators of acute febrile patients with DENV, *Plasmodium,* bacteria (*Neisseria meningitidis* and GAS) and unknown infections. **(a)** Conditional inference tree analysis on serum concentrations of eight disease-specific cytokines from infected patients of DENV (n = 100), *Plasmodium* (PLAS; n = 30), *N. meningitidis* (N.MEN; n = 21), group A streptococcus (GAS; n = 26) and patients with febrile unknown diseases (FUD; n = 30) resulted in an optimum immune signature comprising six cytokines (MIP-1α, TNF-α, GRO-α, RANTES, SDF-1α and PIGF-1) with overall classification accuracy of 68.6%. The cytokines are displayed in square nodes. Numbers between nodes indicate Log_{10} concentration of cytokine in pg mL^{-1} for each split. Each node in conditional inference tree represents a decision to go down one branch or the other depending upon the cut-off values depicted along the line connecting the successive nodes. Finally, each sample ends up in one of the terminal nodes. Terminal nodes display the relative proportion of samples from DENV (light green), *Plasmodium* (teal), bacterial (red) and febrile unknown (orange) infections. **(b)** Radar chart summarising the signature of six immune mediators from conditional inference tree. Serum concentrations for each immune mediator were graphed on separate axes, with all axes being scaled equally from 0% to 100%.

METHODS

Ethical approval

Written informed consent was obtained from all participants, participants' parents or legal guardians, and the study was conducted according to Declaration of Helsinki principles. The collection of samples was approved by the Ethical Committee Panel with IRB number 17/EA/002/1436H in King Fahad Central Hospital, Jazan, Saudi Arabia.

Study participants

A total of 2018 febrile patients admitted to the infectious diseases clinic (IDC) at King Fahad Central Hospital between January 2014 and December 2017 enrolled in the study. Full personal details of patients including recent travel history and exposure to mosquitoes, and detailed clinical histories and clinical examinations were recorded. The patients in this study did not have severe disease outcomes. Thirty-one healthy donors, who were staff at King Fahad Central Hospital, were also recruited as control participants.

Sample collection and patient diagnosis

Acute-phase (within 7 days post-illness onset) blood and serum samples were collected from patients upon hospital admission. With the diagnostic tests available in the hospital, samples from both patients and healthy donors were processed and tested for seven febrile-related pathogens: DENV, CHIKV, *Plasmodium*, *Brucella*, *N. meningitidis*, GAS and *Leptospira*. Confirmatory investigations for acute DENV infection include PCR and ELISAs for NS1 antigen detection (Bio-Rad Laboratories, Inc., Hercules, CA, USA) and IgM and IgG quantifications (Bioactiva Diagnostica GmbH, Bad Homburg, Germany). For CHIKV diagnosis, PCR and ELISAs for IgM and IgG quantifications (EUROIMMUN AG, Lübec, Germany) were performed. Bacterial infections were identified by traditional culture methods. Immunochromatographic test (ICT malaria p.f/p.v) and thick and thin blood films were used for confirmation of acute malaria infection.

Laboratory analysis

Routine laboratory tests were carried out for all participants. Complete blood count, haemoglobin level, lymphocyte and neutrophil percentages, platelet (PLT) count, CRP level, ESR and liver enzymes AST and ALT were quantified with automated haematology and blood chemistry analysers.

Multiplex microbead-based immunoassay

Levels of immune mediators from serum samples of DENV-, *Plasmodium*-, *N. meningitidis*- and GAS-infected patients, as well as febrile unknown patients, were measured using the ProcartaPlex Human Cytokine 45-Plex [granulocyte–macrophage colony-stimulating factor (GM-CSF), EGF, BDNF, beta-nerve growth factor (bNGF), basic fibroblast growth factor 2 (FGF-2), hepatocyte growth factor (HGF), monocyte chemoattractant protein-1 (MCP-1/CCL2), macrophage inflammatory protein-1α (MIP-1α/CCL3), MIP-1β, regulated on activation, normal T cell expressed and secreted (RANTES/CCL5), growth-regulated oncogene-α (GRO-α/CXCL1), stromal cell-derived factor-1α (SDF-1α/CXCL12α), interferon-γ-induced protein 10 kDa (IP-10/CXCL10), eotaxin, interferon-α (IFN-α), IFN-γ, interleukin-1α (IL-1α), IL-1β, IL-1RA, IL-10, IL-13, IL-15, IL-17A, IL-18, IL-2, IL-21, IL-22, IL-23, IL-27, IL-31, IL-4, IL-5, IL-6, IL-7, IL-8 (CXCL8), IL-9, IL-12 p70, leukaemia inhibitory factor (LIF), stem cell factor (SCF), TNF-α, TNF-β, vascular endothelial growth factor A (VEGF-A), VEGF-D, PDGF-BB and placental growth factor-1 (PlGF-1)] immunoassay kits (Thermo Fisher Scientific, Waltham, MA, USA) according to manufacturer's instructions as previously described.[54] Briefly, magnetic beads were aliquoted in 96-well plates followed by addition of standards and sera from patients and control subjects. After an incubation period, plates were washed using a magnetic wash station according to manufacturer's instructions, followed with addition of a detection antibody. Plates were incubated for 30 min and washed, followed by an incubation of 10 min in the presence of streptavidin-PE. Results were acquired using the Bio-Plex 200 (Bio-Rad Laboratories, Inc.) with xPONENT® software (Luminex Corporation, Austin, TX, USA) based on standard curves plotted through a 5-parameter logistic curve setting. IFN-α, IL-5 and IL-9 were found to be below detection limit and hence excluded from subsequent analysis.

Data analysis

Sample randomisation for the Luminex assays could not be performed for the various sample groups as the processing of the samples was dependent on the collection at the hospital. Once sufficient samples were collected, the Luminex assays were performed. To remove any potential plate effects, an additional plate was assayed which contained a selected number of samples from all assayed plates. These samples were then used to normalise the assayed plates. A correction factor was obtained from the difference observed between the original assayed plate data and the replicates on the additional plate. This correction factor was then applied to the rest of the samples of the original assayed plate. The concentrations were logarithmically transformed to ensure normality. One-way ANOVA with the post hoc test corrected using the method of Bonferroni was used to detect for differences between the various sample groups. One-way ANOVA results were corrected for multiple testing using the method of Benjamini and Hochberg. *P*-values < 0.05 were considered to be statistically significant. Plots were generated using GraphPad Prism version 7 (GraphPad Software, San Diego, CA, USA).

Receiver operating characteristic curve analysis for analytes that were differentially expressed between pathogen-infected patients and healthy controls was performed, and the AUCs were calculated. Analytes with AUCs of > 0.65, and specificity and sensitivity values of > 0.70 are considered to be potential markers of disease-specific infections. Conditional inference tree analysis and radar plots of immune mediators of interest were analysed using the R party package (R Foundation for Statistical Computing, Vienna, Austria). The conditional tree was generated with a 10-fold cross-validation to avoid overfitting of data.

ACKNOWLEDGMENTS

We thank the study participants and healthy volunteers for their participation, and clinical staffs from King Fahad Central Hospital for assistance in patient enrolment and care, blood sample preparation, study coordination and data entry. This work is supported by core research grants provided to the Singapore Immunology Network by the Biomedical Research Council (BMRC) and Immunomonitoring Service Platform (grant #NRF2017_SISFP09). The funders had no role in study design, data collection and analysis, decision to publish or preparation of the manuscript.

AUTHOR CONTRIBUTIONS

Yiu-Wing Kam: Data curation; Investigation; Visualization; Writing-original draft. **Mohamed Yousif Ahmed:** Data curation; Investigation; Resources; Writing-original draft. **Siti Naqiah Amrun:** Visualization; Writing-original draft; Writing-review & editing. **Bernett Lee:** Formal analysis; Visualization; Writing-review & editing. **Tarik Refaie:** Data curation; Investigation; Resources. **Kamla Elgizouli:** Data curation;

Investigation; Resources. **Siew-Wai Fong:** Visualization; Writing-original draft; Writing-review & editing. **Laurent Renia:** Conceptualization; Funding acquisition; Writing-review & editing. **Lisa FP Ng:** Conceptualization; Funding acquisition; Project administration; Resources; Writing-original draft; Writing-review & editing.

CONFLICT OF INTEREST

The authors declare no conflict of interests.

REFERENCES

1. Shibl A, Senok A, Memish Z. Infectious diseases in the Arabian Peninsula and Egypt. *Clin Microbiol Infect* 2012; **18**: 1068–1080.
2. Al-Tawfiq JA, Memish ZA. Mass gathering medicine: 2014 Hajj and Umra preparation as a leading example. *Int J Infect Dis* 2014; **27**: 26–31.
3. Aloufi AD, Memish ZA, Assiri AM, McNabb SJN. Trends of reported human cases of brucellosis, Kingdom of Saudi Arabia, 2004–2012. *J Epidemiol Glob Health* 2016; **6**: 11–18.
4. Al-Eissa YA. Brucellosis in Saudi Arabia: past, present and future. *Ann Saudi Med* 1999; **19**: 403–405.
5. Memish Z. Brucellosis control in Saudi Arabia: prospects and challenges. *J Chemother* 2001; **13**: 11–17.
6. Borrow R, Caugant DA, Ceyhan M *et al*. Meningococcal disease in the Middle East and Africa: findings and updates from the Global Meningococcal Initiative. *J Infect* 2017; **75**: 1–11.
7. Borrow R, Lee JS, Vázquez JA *et al*. Meningococcal disease in the Asia-Pacific region: findings and recommendations from the Global Meningococcal Initiative. *Vaccine* 2016; **34**: 5855–5862.
8. Yezli S, Assiri AM, Alhakeem RF, Turkistani AM, Alotaibi B. Meningococcal disease during the Hajj and Umrah mass gatherings. *Int J Infect Dis* 2016; **47**: 60–64.
9. Al-Khadidi FJ, AlSheheri MA, AlFawaz TS, Enani MA, AlAqeel AA, AlShahrani DA. Group A Streptococcal bacteraemia: experience at King Fahad Medical City in Riyadh. *Saudi Arabia. Saudi Med J* 2017; **38**: 1034–1037.
10. Ralph AP, Carapetis JR. Group A streptococcal diseases and their global burden. *Curr Top Microbiol Immunol* 2013; **368**: 1–27.
11. O'Brien KL, Beall B, Barrett NL *et al*. Epidemiology of invasive Group A *Streptococcus* disease in the United States, 1995–1999. *Clin Infect Dis* 2002; **35**: 268–276.
12. Stockmann C, Ampofo K, Hersh AL *et al*. Evolving epidemiologic characteristics of invasive Group A streptococcal disease in Utah, 2002–2010. *Clin Infect Dis* 2012; **55**: 479–487.
13. Esmaeili S, Naddaf SR, Pourhossein B *et al*. Seroprevalence of Brucellosis, Leptospirosis, and Q Fever among butchers and slaughterhouse workers in South-Eastern Iran. *PLoS One* 2016; **11**: e0144953.
14. Bharti AR, Nally JE, Ricaldi JN *et al*. Leptospirosis: a zoonotic disease of global importance. *Lancet Infect Dis* 2003; **3**: 757–771.
15. Bukhari H. An unusual cause of hemoptysis in a young male patient. *J Taibah Univ Med Sci* 2007; **2**: 50–55.
16. Salam N, Mustafa S, Hafiz A, Chaudhary AA, Deeba F, Parveen S. Global prevalence and distribution of coinfection of malaria, dengue and chikungunya: a systematic review. *BMC Public Health* 2018; **18**: 710.
17. Kilpatrick AM, Randolph SE. Drivers, dynamics, and control of emerging vector-borne zoonotic diseases. *Lancet* 2012; **380**: 1946–1955.
18. Coleman M, Al-Zahrani MH, Coleman M *et al*. A country on the verge of malaria elimination - the Kingdom of Saudi Arabia. *PLoS One* 2014; **9**: e105980.
19. Hawash Y, Ismail K, Alsharif K, Alsanie W. Malaria prevalence in a low transmission area, Jazan district of southwestern Saudi Arabia. *Korean J Parasitol* 2019; **57**: 233–242.
20. Snow RW, Amratia P, Zamani G *et al*. The malaria transition on the Arabian Peninsula: Progress toward a malaria-free region between 1960–2010. *Adv Parasitol* 2013; **82**: 205–251.
21. Fakeeh M, Zaki AM. Virologic and serologic surveillance for dengue fever in Jeddah, Saudi Arabia, 1994–1999. *Am J Trop Med Hyg* 2001; **65**: 764–767.
22. Alhaeli A, Bahkali S, Ali A, Househ MS, El-Metwally AA. The epidemiology of dengue fever in Saudi Arabia: a systematic review. *J Infect Public Health* 2016; **9**: 117–124.
23. Hussain R, Alomar I, Memish ZA. Chikungunya virus: emergence of an arthritic arbovirus in Jeddah. *Saudi Arabia. East Mediterr Health J* 2013; **19**: 506–508.
24. Mattar S, Alvis N, Gonzalez M.Haemorrhagic fevers transmitted by vectors in the neotropics. In: Rodriguez-Morales AJ (ed). *Current Topics in Public Health*. London: Intech, 2013, pp. 381–4001. https://doi.org/10.5772/55420
25. Mattar S, Tique V, Miranda J, Montes E, Garzon D. Undifferentiated tropical febrile illness in Cordoba, Colombia: not everything is dengue. *J Infect Public Health* 2017; **10**: 507–512.
26. Aguilar PV, Estrada-Franco JG, Navarro-Lopez R, Ferro C, Haddow AD, Weaver SC. Endemic Venezuelan equine encephalitis in the Americas: hidden under the dengue umbrella. *Future Virol* 2011; **6**: 721–740.
27. Huang C, Wang Y, Li X *et al*. Clinical features of patients infected with 2019 novel coronavirus in Wuhan, China. *Lancet* 2020; **395**: 497–506.
28. Altassan KK, Morin C, Shocket MS, Ebi K, Hess J. Dengue fever in Saudi Arabia: a review of environmental and population factors impacting emergence and spread. *Travel Med Infect Dis* 2019; **30**: 46–53.
29. Beck-Johnson LM, Nelson WA, Paaijmans KP, Read AF, Thomas MB, Bjørnstad ON. The effect of temperature on Anopheles mosquito population dynamics and the potential for malaria transmission. *PLoS One* 2013; **8**: e79276.
30. Malik MR, Mnzava A, Mohareb E *et al*. Chikungunya outbreak in Al-Hudaydah, Yemen, 2011: epidemiological characterization and key lessons learned for early detection and control. *J Epidemiol Glob Health* 2014; **4**: 203–211.
31. Rezza G, El-Sawaf G, Faggioni G *et al*. Co-circulation of dengue and chikungunya viruses, Al Hudaydah, Yemen, 2012. *Emerg Infect Dis* 2014; **20**: 1351–1354.
32. Taraphdar D, Sarkar A, Mukhopadhyay BB, Chatterjee S. A comparative study of clinical features between monotypic and dual infection cases with chikungunya virus and dengue virus in West Bengal. *India. Am J Trop Med Hyg* 2012; **86**: 720–723.

33. Singh J, Dinkar A, Singh RG, Siddiqui MS, Sinha N, Singh SK. Clinical profile of dengue fever and coinfection with chikungunya. *Ci Ji Yi Xue Za Zhi = Tzu-chi Med J* 2018; **30**: 158–164.
34. Azin FRFG, Gonçalves RP, Pitombeira MH, Lima DM, Branco IC. Dengue: profile of hematological and biochemical dynamics. *Rev Bras Hematol Hemoter* 2012; **34**: 36–41.
35. Mourão MPG, Lacerda MVG, Macedo VO, Santos JB. Thrombocytopenia in patients with dengue virus infection in the Brazilian Amazon. *Platelets* 2007; **18**: 605–612.
36. Al-Gwaiz LA, Babay HH. The diagnostic value of absolute neutrophil count, band count and morphologic changes of neutrophils in predicting bacterial infections. *Med Princ Pract* 2007; **16**: 344–347.
37. Demissie DE, Kaplan SL, Romero JR *et al*. Altered neutrophil counts at diagnosis of invasive meningococcal infection in children. *Pediatr Infect Dis J* 2013; **32**: 1070–1072.
38. Lee YH, Leong WY, Wilder-Smith A. Markers of dengue severity: a systematic review of cytokines and chemokines. *J Gen Virol* 2016; **97**: 3103–3119.
39. Angulo I, Fresno M. Cytokines in the pathogenesis of and protection against malaria. *Clin Diagn Lab Immunol* 2002; **9**: 1145–1152.
40. Spain-Santana TA, Marglin S, Ennis FA, Rothman AL. MIP-1α and MIP-1β induction by dengue virus. *J Med Virol* 2001; **65**: 324–330.
41. Lee YR, Liu MT, Lei HY *et al*. MCP1, a highly expressed chemokine in dengue haemorrhagic fever/dengue shock syndrome patients, may cause permeability change, possibly through reduced tight junctions of vascular endothelium cells. *J Gen Virol* 2006; **87**: 3623–3630.
42. Rathakrishnan A, Wang SM, Hu Y *et al*. Cytokine expression profile of dengue patients at different phases of illness. *PLoS One* 2012; **7**: e52215.
43. Guabiraba R, Ryffel B. Dengue virus infection: current concepts in immune mechanisms and lessons from murine models. *Immunology* 2014; **141**: 143–156.
44. Clark IA. Along a TNF-paved road from dead parasites in red cells to cerebral malaria, and beyond. *Parasitology* 2009; **136**: 1457–1468.
45. Castellon R, Hamdi HK, Sacerio I, Aoki AM, Kenney MC, Ljubimov AV. Effects of angiogenic growth factor combinations on retinal endothelial cells. *Exp Eye Res* 2002; **74**: 523–535.
46. Bafadhel M, Haldar K, Barker B *et al*. Airway bacteria measured by quantitative polymerase chain reaction and culture in patients with stable COPD: Relationship with neutrophilic airway inflammation, exacerbation frequency, and lung function. *Int J Chron Obstruct Pulmon Dis* 2015; **10**: 1075–1083.
47. Hoenderdos K, Condliffe A. The neutrophil in chronic obstructive pulmonary disease. *Am J Respir Cell Mol Biol* 2013; **48**: 531–539.
48. Alam R, Stafford S, Forsythe P *et al*. RANTES is a chemotactic and activating factor for human eosinophils. *J Immunol* 1993; **150**: 3442–3448.
49. Matthews AN, Friend DS, Zimmermann N *et al*. Eotaxin is required for the baseline level of tissue eosinophils. *Proc Natl Acad Sci USA* 1998; **95**: 6273–6278.
50. Young BE, Ong SWX, Ng LFP *et al*. Immunological and viral correlates of COVID-19 disease severity: a prospective cohort study of the first 100 patients in Singapore. *SSRN Electron J* 2020. e-pub ahead of print 20 May 2020. https://doi.org/10.2139/ssrn.3576846
51. Qin C, Zhou L, Hu Z *et al*. Dysregulation of immune response in patients with Coronavirus 2019 (COVID-19) in Wuhan, China. *Clin Infect Dis* 2020: ciaa248. e-pub ahead of print 12 March 2020. https://doi.org/10.1093/cid/ciaa248
52. Liu J, Li S, Liu J *et al*. Longitudinal characteristics of lymphocyte responses and cytokine profiles in the peripheral blood of SARS-CoV-2 infected patients. *EBioMedicine* 2020; **55**: 102763.
53. Chen G, Wu D, Guo W *et al*. Clinical and immunological features of severe and moderate coronavirus disease 2019. *J Clin Invest* 2020; **130**: 2620–2629.
54. Kam Y-W, Leite JA, Lum F-M *et al*. Specific biomarkers associated with neurological complications and congenital central nervous system abnormalities from Zika virus-infected patients in Brazil. *J Infect Dis* 2017; **216**: 172–181.

Supporting Information

Additional supporting information may be found online in the Supporting Information section at the end of the article.